PHYSICAL REVIEW D **83**, 103520 (2011)

Quark matter induced extensive air showers

Kyle Lawson
Department of Physics and Astronomy, University of British Columbia, Vancouver, BC, V6T 1Z1, Canada
(Received 13 December 2010; published 19 May 2011)

If the dark matter of our Galaxy is composed of nuggets of quarks or antiquarks in a color superconducting phase there will be a small but nonzero flux of these objects through the Earth's atmosphere. A nugget of quark matter will deposit only a small fraction of its kinetic energy in the atmosphere and is likely to be undetectable. If however the impacting object is composed of antiquarks, the energy deposited can be quite large. In this case nuclear annihilations within the nugget will trigger an extensive air shower the particle content of which is similar to that produced by an ultrahigh energy cosmic ray. This paper gives a qualitative description of the basic properties of such a shower. Several distinctions from an air shower initiated by a single ultrahigh energy nucleus will be described, allowing these events to be distinguished from the cosmic ray background. The subtlety of these features may mean that some fraction of the high energy cosmic ray spectrum may in fact be due to this type of dark matter interaction. The estimated flux of dark matter nuggets and the energy deposited in the atmosphere are such that the Pierre Auger Observatory may prove an ideal facility to place constraints on the flux of heavy quark matter objects. This paper attempts to highlight the best techniques to search for a quark matter signature through an extensive air shower signal.

DOI: 10.1103/PhysRevD.83.103520 PACS numbers: 95.35.+d, 12.38.Mh, 98.70.Rz

I. INTRODUCTION

A. Quark matter as a dark matter candidate

It has been suggested that dark matter may be composed of macroscopically large, strongly interacting, composite objects comprised of light quarks of the standard model in a nonbaryonic phase such as strange quark matter [1] or a color superconducting phase [2]. In the latter case the composite objects may be bound states of either quarks or antiquarks which are stable over cosmological time scales. While strongly interacting these objects remain ''dark'' due to their large mass to surface area ratio and the correspondingly low number density required to explain the observed dark matter mass density. The total baryonic charge of the composite object is the dominant uncertainty in this model as it depends on the poorly understood physics of nugget formation (which occurs at the QCD phase transition). A combination of theoretical and observational constraints suggests that the mean baryonic charge must exceed 10^{20} [2] while the upper bound is dependent on the formation model and is not well constrained.

A brief qualitative overview of the structure of a quark nugget is given in Appendix A. Further, more precise, details of various phases of quark matter are available in the references given there.

Previous works have studied the observational consequences of the presence of quark matter within the Galaxy. No contradictions are found with existing observations; in fact the emission produced by these objects may help to explain several anomalies in the galactic spectrum such as the strong 511 keV line [3–5], the COMPTEL excess at 10 MeV [6,7], the diffuse x-ray background [8,9], and the WMAP ''haze'' [10,11]. Based on the simplest models of the dark matter distribution and nugget interaction with the interstellar medium a best fit to the galactic spectrum in this analysis is found to favor a baryonic charge for the nuggets of $B \sim 10^{25}$.

B. Extensive air showers from quark matter

The cosmic ray spectrum is now observed to extend to energies above 10^{20} eV [12]. The incredibly small flux of cosmic rays at these energies requires a correspondingly large detector to obtain useful statistics for these events. The aim of this work is to highlight the possibility that these detectors can also impose significant constraints on massive composite dark matter candidates. Composite objects composed purely of matter will deposit only a fraction of their kinetic energy in the atmosphere. The small energy scales involved do not allow for substantial particle generation and make direct detection unlikely. However, in the case of a nugget composed of antimatter the dominant interactions between the atmosphere and antiquark matter will be strong force mediated matter-antimatter annihilations. The hadronic shower resulting from these annihilations will be dominated by light mesons and their decay products. The energy deposited by such an event will be considerably larger than the nugget's kinetic energy and the resulting shower should be readily observable. As in the case of a single ultrahigh energy proton or ion a quark

*klawson@phas.ubc.ca

nugget impacting the Earth's atmosphere will be observable through the extensive air shower which develops around the primary particle. However, in the model considered here the shower is driven not by the kinetic energy of the primary but by the energy released in matter-antimatter annihilations. This makes these events fundamentally different than the previously considered cases of highly accelerated dust or strangelets [13]. Existing models of cosmic rays require an accelerator capable of providing sufficient kinetic energy for the primary particle to trigger an extensive air shower; in the present case no such accelerator is required as the shower is driven by energy released in nuclear annihilations. This allows a large air shower to develop despite the fact that the primary particle has a relatively small (galactic scale) velocity.

This paper gives an overview of the process by which a quark nugget deposits energy in the atmosphere and the properties of the resulting extensive air shower. As in the case of an air shower initiated by a single ultrahigh energy cosmic ray these quark matter induced showers arise through a very large number of hadronic interactions which necessarily cascade down to similar final state products. As such the particle content of the shower, as observed at the Earth's surface, will be quite similar to that of a conventional shower. A detailed description of the resulting air shower would require large scale numerical simulations (similar to those conducted for proton or nuclei initiated showers) which are beyond the scope of this work. In an attempt to keep the physical picture as clear as possible the body of this work focuses on only the most essential features of the shower rather than microscopic details which may be strongly dependent on the precise structure of the strong interactions at large densities. While a quark matter initiated shower is in many ways similar to a cosmic ray air shower there are also several critical differences in both the geometry and the time scales involved. The final section of this work highlights these differences and discusses potential techniques for the detection of quark matter induced air showers.

II. TOTAL FLUX

The exact distribution of dark matter in the Galaxy remains uncertain. Recent simulations indicate the possibility of significant structure at subgalactic scales [14] which could significantly affect the flux of dark matter through the Earth. In the interest of simplicity the following analysis assumes a local density consistent with a smooth density profile and a velocity set by virial equilibrium. Under these assumptions the dark matter density in the neighborhood of our Solar system is $\rho_{\rm DM} \approx 1.5\ \mathrm{GeV/cm^3}$. Assuming that the effective mass of quarks in a color superconductor is comparable to that of hadronic quarks this mass density translates to a number density of nuggets approximately given by $n \sim B^{-1}\mathrm{cm}^{-3}$, where B is the total baryon number of the nuggets. The number density can then be combined with the mean galactic velocity $v_g \sim 200\ \mathrm{km/s}$ to obtain a flux of nuggets at the Earth's surface,

$$\frac{dN}{dAdt} = n v_g \approx (10^{25}\ \mathrm{km}^{-2}\,\mathrm{yr}^{-1})B^{-1}. \tag{1}$$

Based on this order of magnitude estimation nuggets with a baryonic charge distribution near that favored by fits to the galactic spectrum will produce a flux comparable to that of cosmic rays near the Greisen-Zatsepin-Kuzmin (GZK) limit [15,16]. It is precisely this flux range that the Pierre Auger Observatory [17] was designed to study and, consequently, it is also capable of constraining the presence of heavy quark matter in the cosmic ray spectrum. One might also consider looking for a quark nugget signal at large underground detectors however, as discussed in Appendix C, the larger surface area presented by Auger allows it to impose much tighter constraints.

III. ENERGETICS

This section gives an overview of the energy considerations related to a quark nugget induced air shower without focusing on the details of how this energy is deposited in the atmosphere. While an antiquark nugget contains a large amount of antimatter very little of it actually annihilates as the nugget traverses the atmosphere. The annihilation rate is not limited by the nugget's mass but by the rate at which the nugget sweeps up atmospheric matter. This rate is determined by the atmospheric density and the nugget's cross-sectional area. At the Earth's surface the integrated mass of atmospheric molecules is on the order of $1\ \mathrm{kg/cm^2}$ while the nugget radius is generally found to be on the order of 10^{-5} cm. For these values, if all the atmospheric molecules striking the nugget annihilate completely, the energy produced while crossing the atmosphere is

$$\Delta E = 2X_{at}\pi R_n^2 = 10^{26}\ \mathrm{eV}\left(\frac{R_n}{10^{-5}\ \mathrm{cm}}\right)^2. \tag{2}$$

This represents the total energy production from annihilations. The majority of this energy is thermalized within the nugget and will not take a readily observable form. It will also be shown that only a fraction of all molecules incident on the nugget actually annihilate. Thus, the expression (2) represents a maximum energy available to the shower with the actual value likely to be several orders of magnitude smaller.

For comparison the kinetic energy transferred to the atmosphere can be estimated by assuming that all molecules in the atmosphere are accelerated from rest to the typical nugget velocity of 200 km/s

$$\Delta T = \frac{1}{2}X_{at}\pi R_n^2 v_n^2 = 10^{17}\ \mathrm{eV}\left(\frac{R_n}{10^{-5}\ \mathrm{cm}}\right)^2. \tag{3}$$

This is many orders of magnitude below the energy produced by annihilations and represents only a minuscule fraction of the total energy involved. Kinetic energy transfer may accelerate a large number of atmospheric molecules but will be a purely elastic process producing neither new particles nor significant amounts of ionization. For this reason the following discussion will deal with only the shower produced by antimatter nuggets and the energy transferred by inelastic collisions will be ignored.

IV. SHOWER COMPONENTS

As stated above the quark matter induced shower will primarily arise from the annihilation of atomic nuclei within the nugget. The main product of these annihilations will be light mesons (the exact composition of these mesons depends on the form of quark matter realized in the nuggets [18]). Given the relatively low momenta at which they are produced these strongly interacting modes are unlikely to escape across the quark matter surface. Instead, through a complex series of interactions, they will lose energy to the lighter modes of the superconductor. This process results in a collection of excited electromagnetically bound modes as well as thermalizing energy within the nugget. The following sections give a brief overview of the particle content generated in these interactions.

A. Electromagnetic shower

There are three primary mechanisms which will result in the emission of energetic photons from the nugget. First annihilations within the nugget cascade from the initial mesons down to the leptonic modes. As the lightest available energy carriers the positrons within the quark matter absorb the majority of this momentum. A positron incident on the quark matter surface from within the nugget will rapidly decelerate within the strong electric fields at the surface and remain bound to the nugget. This process leads to the emission of x-rays through bremsstrahlung. A second radiation production mechanism involves energetic electrons produced inside the nugget which annihilate with the positrons of the electrosphere. These annihilations, as well as annihilations of the electrons of atmospheric molecules, produce gamma rays with energies up to a few tens of MeV which will be released into the atmosphere. A final photon contribution comes from thermal emission from the surface of the electrosphere. As the nugget heats up due to the increasing rate of annihilations the surface can reach temperatures at the keV scale. This will result in the emission of considerable amounts of thermal radiation. These energetic photon components of the nugget emission spectrum will generate an electromagnetic shower as they ionize the surrounding atmospheric molecules.

B. Muons

As mentioned above the electrons and positrons produced in the nugget are unlikely to be able to escape into the atmosphere. Muons, because of their larger mass, lose energy less efficiently and are able to escape from the nugget's surface. As such they are the dominant charged particles deposited in the atmosphere. Initial muon energies will be determined by the energy scale of the lightest hadronic modes of the color superconductor, typically around a few hundred MeV. Muons that escape the nugget deposit energy in the surrounding atmosphere producing atmospheric fluorescence until they decay. The treatment of muon energy loss to the surrounding atmosphere is described in Appendix B and is important in determining the morphology of the resulting shower.

The exact geometry of muon emission from the nugget is a complex problem. At a basic level the majority of atmospheric molecules first strikes the nugget surface on the downward directed face. The molecules will have relatively little time to migrate across the surface before they penetrate into the quark matter and annihilate. As discussed in [9] the combination of large penetration depth and the rapid energy loss from the jets produced by annihilations within the nugget favors the emission of muons directly perpendicular to the quark matter surface above the point of annihilation. This argument, when combined with the preferential flux of atmospheric material along the axis of the nugget's velocity, implies preferential emission in the forward direction. The simplest model would imply something like a cosine dependence but an exact estimate of this effect would depend on quite complicated material transport properties near the surface. In what follows it will simply be assumed that emission preferentially occurs from the forward directed face of the nugget.

V. NUGGET THERMODYNAMICS

Before proceeding to a more detailed description of a quark nugget induced air shower some basic thermodynamic properties of the nuggets must be introduced. The majority of the energy deposited by nuclear annihilations is thermalized within the nugget. The exact fraction, hereafter labeled f_T, is dependent on the exact details of the quark matter and will not be calculated here. As the annihilations happen at low momenta the products are likely to be emitted without a preferred direction and any energy moving deeper into the nugget will certainly be thermalized. This basic geometric consideration suggests that $1 < f_T < 1/2$ with values near the upper limit more likely.

A. Thermodynamic equilibrium

This thermal energy is eventually radiated from the nugget's surface at the point where the electrosphere becomes transparent to thermal photons. This process was described in [11] where the emission spectrum was found to be

$$\frac{dE}{dtdA} \approx \frac{16}{3} \frac{T^4 \alpha^{5/2}}{\pi} \sqrt{\frac{T}{m_e}}, \tag{4}$$

implying a suppression of thermal emission, with respect to blackbody, at low temperatures. The following analysis assumes that thermalization happens rapidly enough that the nugget remains near thermodynamic equilibrium. Under this assumption the rate at which thermal energy is deposited by annihilations will be equal to the rate at which energy is radiated from the electrosphere. The accretion rate is set by the nugget's velocity and the local atmospheric density and allows the nugget's surface temperature to be determined at a given height,

$$\left(\frac{T}{m_e}\right)^{17/4} = \frac{3\pi\alpha^{1/2}}{64} \frac{a_b^3}{m_e} \rho_{at}(h) v_n f_T = \left(\frac{\rho_{at}(h)}{860 \text{ g/cm}^3}\right)\left(\frac{v_n}{200 \text{ km/s}}\right) f_T. \tag{5}$$

This estimation should remain valid as long as the temperature remains well below the electron mass (which is true over the entire atmosphere). This implies that the temperature of a nugget near the Earth's surface will be around 20 keV provided that all material in the nugget's path is annihilated.

B. Molecular deflection

This section is devoted to determining the maximum rate at which matter can be deposited onto a quark matter surface. Intuitively as the flux of matter onto the nugget's surface increases so must the rate at which the resulting energy is transferred away from the surface. While the exact mechanism by which this energy transfer occurs may be quite complicated any plausible outward transfer of energy will exert a pressure on the incoming matter and limit the rate at which it can be fed onto the quark surface. This negative feedback suggests that there will be a density beyond which the annihilation rate saturates. The following analysis attempts to be as general as possible to extract a generic scale at which matter annihilation rates reach a maximum.

As demonstrated in [19], electron-positron annihilations at low temperature are dominated by the formation of an intermediate positronium state. Positronium formation is a resonance process with a probability near 1 at low momenta but which falls off rapidly as the center of mass momentum of the collision is increased. If the momentum is substantially larger that the positronium binding energy ($2m_e\alpha$) then the probability of forming a positronium bound state becomes negligible. This happens very high in the atmosphere so that the primary annihilation channel at relevant atmospheric densities is the direct $e^+e^- \rightarrow 2\gamma$ process described in [7]. At temperatures below the electron mass this process is actually less efficient than elastic scattering. In this case many positrons will scatter off of the incoming molecule before any of the electrons annihilate. The incoming molecules carry a kinetic energy $T_{at} = \frac{1}{2}M_{at}v^2$; for a nitrogen molecule striking the nugget at 200 km/s this energy is a few keV. As the temperature increases each positron scattering transfers more energy until the energy transfer becomes sufficient to deflect the incident molecule. The exact temperature at which this occurs is dependent on the exact details of energy transfer within the electrosphere and will not be determined here. Instead the following analysis will simply assume that the temperature must be slightly above the kinetic energy of the incoming molecule.

VI. FLUORESCENCE PROFILE

This section attempts to map the thermodynamic evolution described above onto a physical description of the resulting air shower. The atmospheric fluorescence yield of a shower is determined primarily from the number of charged particles moving through the atmosphere at a given point. These particles lose energy to the surrounding atmosphere exciting nitrogen molecules which subsequently radiate in the UV band.

The fraction of muons per annihilated nucleon which escapes the nugget depends on the precise details of the quark matter surface and on the mass of the lightest mesons in the dense quark matter (the decay of these being the primary muon production channel). In vacuum $p\bar{p}$ annihilations produce a large number of pions. The uncharged π^0s decay to photons while the charged pions decay to muons. As such an annihilation in vacuum typically yields between four and six muons. This should be taken as the upper limit for total muon production per nucleon annihilated though only a fraction of these muons manages to escape the nugget. Thus, the rate of muon production per annihilated nucleon, χ_μ, has a maximum possible value of order 1 while the actual value may be substantially lower. The uncertainty in χ_μ is sufficient that the magnitude of the fluorescence yield is only weakly constrained at the present level of analysis.

A. Geometry

In Sec. V B it was argued that there must be a temperature at which the nuclear annihilation rate saturates. If this happens at a nugget surface temperature $T_{\max}$ then this rate may be found from expression (4),

$$\frac{dN}{dt} = \frac{32}{3} R_n^2 \alpha^{5/2} \frac{T_{\max}^4}{m_p} \sqrt[4]{\frac{T_{\max}}{m_e}} \approx 2 \times 10^{17} \text{ s}^{-1} \left(\frac{R_n}{10^{-5} \text{ cm}}\right)\left(\frac{T_{\max}}{10 \text{ keV}}\right)^{17/4}. \tag{6}$$

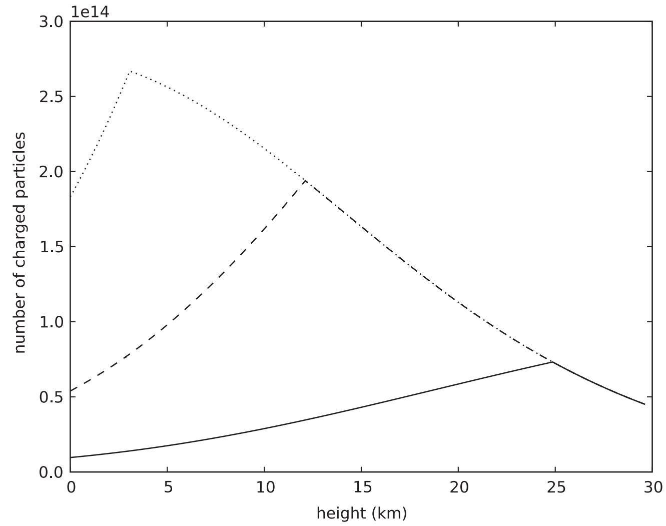

FIG. 1. Muon content of a quark matter initiated shower as a function of height. The curves are for saturation temperatures of 10 keV (solid), 15 keV (dashed), and 20 keV (dotted).

Once this saturation point has been reached the decrease in the mean free path of an emitted particle with increasing atmospheric density implies that the flux of charged particles will decrease with atmospheric depth. The resulting shower profile, using the crude muon propagation model of B is shown in Fig. 1. It should be noted that the overall normalization of Fig. 1 is highly uncertain as it depends on both the muon production rate χ_μ and the mean energy with which muons escape the surface. Neither of these quantities are constrained beyond rough order of magnitude estimates. Rather it is the overall geometry of Fig. 1 that is relevant.

The initial rise in muon flux is due to the increasing rate of nuclear annihilations with atmospheric density. The maximum charged particle number occurs near the point where the annihilation rate saturates and, as the atmospheric density increases beyond this point, its main effect is to decrease the mean free path of a traveling muon. This results in a more rapid loss of muons from the shower and thus a decrease in the integrated charged particle flux.

B. Timing

This basic shower geometry, growing to a maximum particle content then decreasing rapidly beyond that maximum, is similar to that associated with an ultrahigh energy cosmic ray shower, however the fluorescence timing will be substantially different. This difference arises due to the relatively small velocity of the nugget as compared to an ultra high energy cosmic ray. The latter travels at the speed of light while the nuggets have typical galactic velocities, on the order of a few hundred kilometers per second, some 3 orders of magnitude slower.

In both cases the secondary particles, produced in hadronic interactions, move outward at nearly the speed of light. As discussed in Appendix B the charged particles of a quark matter induced shower are generally confined to a region within a few kilometers of the nugget due to their relatively small boost factors. The charged particles spread through this volume over the course of tens of microseconds. However, the illuminated region of atmospheric fluorescence will track with the nugget as it moves through the atmosphere with the shower front advancing quite slowly. The time scales for the progress of the nugget itself will be on the order of a tenth of a second.

The long duration of the atmospheric fluorescence and the large photon multiplicity at any given time make these events very difficult to observe above the various backgrounds. For this reason the fluorescence detector of the Pierre Auger Observatory is unlikely to trigger on a quark nugget air shower [20]. The difficulties inherent in detecting these fluorescence events likely favors searches based on surface detectors.

VII. LATERAL SURFACE PROFILE

When the shower reaches the Earth's surface it will be tightly clustered around the nugget with only the highest energy shower components able to travel far from the shower core. As with the fluorescence profile the exact details of the lateral profile are dependent on models of muon propagation through the atmosphere. Again the results described here are based on the approximations of Appendix B which intends only to capture the most general features of the shower.

As the majority of muons are emitted at relatively low ($\sim$ 10 MeV) energies they are unable to travel far from the nugget in the dense lower atmosphere. However, the shower also contains a smaller number of high energy muons able to travel a larger distance from the nugget.

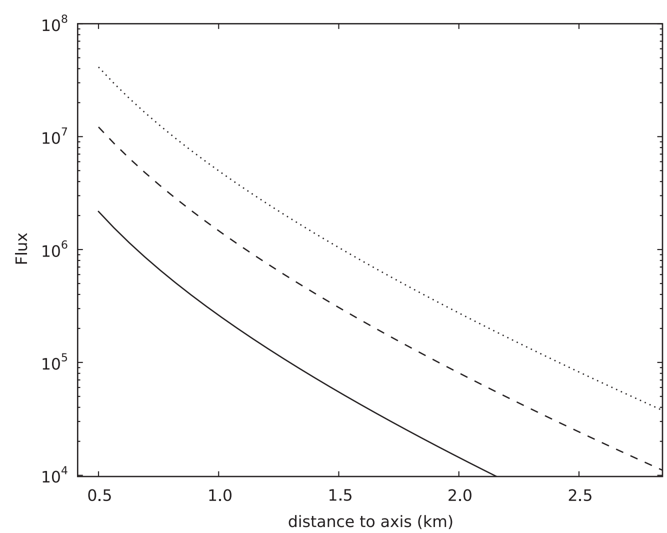

FIG. 2. Particle flux per m^2 as a function of distance from the shower core. The curves are for saturation temperatures of 10 keV (solid), 15 keV (dashed), and 20 keV (dotted).

These higher energy muons produce an extended lateral distribution of particles at the surface. An approximate lateral profile of the shower is plotted in Fig. 2. As with the fluorescence profile the total flux may be rescaled by slight changes in the muon production rate and spectrum. The scaling of Fig. 2 is therefore less significant than the general profile shape. The essential feature of the radial surface profile is a strong peak near the point where the nugget strikes the ground and an exponential drop off with radial distance from this point. The controlling scale for the exponential falloff is determined by the mean free path of a muon averaged over the allowed initial energy scales as described in Appendix B. Numerically it is found that this scale is in the range from a few hundred meters up to a few kilometers for the muon spectra given.

Time scales

As with the fluorescence profile described above, the surface particle distribution is similar in geometry to that of an air shower initiated by a single high energy cosmic ray. But, once again, the timing signature will be very different. In the case of a conventional air shower the particles (primarily muons) arrive at the surface within a time scale of less than a microsecond. This is particularly true of the strongly beamed particles quite near the shower core while the arrival times of particles far from the shower core show considerably more scatter.

In the case of a quark nugget initiated shower the time scale for particle arrival is determined by how long it takes the nugget to pass through the region from which the emitted muons are able to reach the surface. As discussed above the critical length scale for muon propagation is on the order of several hundred meters. For a nugget moving at 200 km/s this implies a shower duration on the order of several milliseconds, several orders of magnitude slower than the duration of an ultrahigh energy primary initiated shower.

Near the shower core the difference in timing signatures between an ultrahigh energy cosmic ray shower and a quark nugget shower will be very clear. However, in the case of an off axis shower the situation is less clear. At larger radial distances the secondary particles of a cosmic ray shower are less strongly beamed and have undergone a larger number of scatterings resulting in a longer shower duration. The opposite is true in the case of a quark nugget induced air shower. In this case it is only the highest energy muons that can travel far from the shower core and the shower duration may be significantly shorter than near the shower core.

VIII. COMPARISON WITH CONVENTIONAL SHOWERS

To this point emphasis has been placed on the similarities between the air shower induced by an antiquark nugget and one produced by a single ultrahigh energy primary. There are however several important distinguishing features between the two. The most important of these arise from the much lower velocity of the primary particle.

(i) A longer shower duration will be observable in atmospheric fluorescence producing an extended fluorescence track which lasts for a longer time.

(ii) The lower velocity of the primary particles will result in a correlation between the arrival direction and the direction of Earth's motion with respect to the Galaxy. This effect produces both seasonal variation (similar to that searched for in the DAMA experiment [21]) as well as a correlation with the direction of motion around the Galactic center.

(iii) The arrival direction of quark nuggets is determined by the local dark matter distribution and, as such, should show no correlation with galactic or nearby intergalactic objects. The presence of a quark matter component in the cosmic ray spectrum would thus dilute any existing correlation with the source of typical ultrahigh energy cosmic rays.

(iv) A distinguishing feature unrelated to the primary particle's velocity is that shower evolution is dependent on the surface temperature of the nugget. As may be seen in Eq. (5) this scales with the atmospheric density rather than the atmospheric depth of the shower. Conversely the evolution of a conventional shower is determined purely by the amount of atmospheric material through which the shower has propagated. A possible consequence of this effect would be a larger apparent depth of maximum for steeply inclined showers. However, without a detailed description of the thermal physics of the nuggets it is possible that the statistical variation in the saturation temperature may be large enough to obscure this effect.

(v) A final distinguishing feature is observable in muon spectroscopy. In both cases the majority of particles will be generated via the decay of pions with QCD scale energies however an ultrahigh energy primary may produce a number of muons with energies well above this scale. Conversely the QCD scale sets the highest energy available to individual particles in a quark nugget initiated shower. An analysis of the muon spectrum at the surface will thus show a high energy cutoff around a GeV in the case of a quark nugget initiated shower while a conventional shower will show no such cutoff.

IX. CONCLUSION AND DISCUSSION

The main purpose of this work has been to point out that large surface area cosmic ray detectors are also well suited to search for the presence of dark matter in the form of quark nuggets. The impact of an antiquark nugget on the atmosphere will produce an extensive air shower consisting of a large number of secondary particles observable through both their impact on surface detectors and the atmospheric fluorescence they generate. The resulting air shower is morphologically similar to one generated by a single ultrahigh energy primary particle in both the fluorescence profile and the lateral distribution at the Earth's surface. It is therefore possible that some part of the high energy cosmic ray spectrum may arise from the partial annihilation of dark matter in the form of heavy quark nuggets.

The exact location of the shower maximum is dependent on rather complicated thermal physics in the electrosphere of the nuggets and, as such, cannot be explicitly formulated in the preliminary treatment presented here and will be the subject of future work. From this analysis it is only possible to argue that there must be an atmospheric density at which thermal pressure overcomes the kinetic energy of atmospheric molecules causing the annihilation rate to saturate. This effect leads to a nontrivial height at which the shower will have a maximum particle content. In this context the observed break in the energy spectrum $10^{19.5}$ eV [12] imposes limits on the total particle content and saturation temperature of the quark nugget.

Finally it should be highlighted that additional work is needed on the atmospheric propagation of particles within this model. While the required simulations are simplified by the absence of very high energy interactions (the properties of which are not well established) the injection of particles is dramatically different from a conventional shower. This requires a fundamentally different formulation of the shower simulations from those presently employed. Without such simulations the extraction of statistical properties of the showers is not possible.

ACKNOWLEDGMENTS

Parts of this work were motivated by early discussions with Brian Fick. I would also like to thank Stéphane Coutu for many useful comments and Ariel Zhitnitsky for his helpful discussions. This research was supported in part by the Natural Sciences and Engineering Research Council of Canada.

APPENDIX A: QUARK NUGGET STRUCTURE

As alluded to above there are several possible phases of quark matter from which the nuggets may be formed. Rather than performing detailed calculations within the context of a particular model this paper will rely only on general properties of quark matter. Reviews of these ideas are available in several previous works such as [22–24]. This appendix will present only the minimal details necessary for the discussion of the phenomenology of quark nugget initiated air showers.

The nuggets have a density at the nuclear scale and may have a lower binding energy than the iron nucleus. If this is the case nuggets formed in the early Universe will be stable over cosmological time scales.

Of particular interest here is the proposal of [2] in which the nuggets may be composed of both matter and antimatter. The preferential formation of antinuggets has been proposed as a mechanism for baryogenesis [25]. In this model the formation of antinuggets is favored by a factor of 3:2 so that, beginning from a universe with no net baryonic charge, antimatter is preferentially hidden in the dark matter nuggets [25].

At asymptotically large densities quark matter is composed of equal numbers of u, d, and s quarks and is charge neutral. However, the large s quark mass results in a depletion of s quarks in lower density quark matter. Even if the bulk of the nugget is charge neutral the decreasing density near the quark surface results in a depletion of s quarks and gives the quark matter a net charge, positive in the case of a matter nugget and negative in the case of an antinugget. To maintain charge neutrality the quark matter is surrounded by a layer of leptons. These leptons are only electromagnetically bound to the surface and extend beyond the quark surface. The exact structure of this layer, known as the electrosphere, was worked out in [19]. Near the quark matter surface the electrons (or positrons) are tightly bound and at nuclear densities however the density falls off with distance down the atomic scale. The presence of a large atomic density shell of positrons surrounding the nugget will play a critical role in interaction between the nugget and molecules of the atmosphere. This layer also determines the thermal properties of the nugget as it is the point where the nugget first becomes transparent to low energy thermal photons.

APPENDIX B: MUON PROPAGATION

This appendix gives a brief description of the approximations made in describing the evolution of the air shower. While the model used is very simple it is intended only for demonstrative purposes and highlights only the most basic properties of the shower. As described above, the only charged particles capable of escaping the quark nugget are muons. The main muon production channel is the decay of a mesonlike excitation which will produce muons with energies at the GeV scale. These muons rapidly lose energy in subsequent scatterings, primarily with the positrons which are the lightest available modes. Energy loss will continue until the momentum of the muon is on the same scale as the plasma frequency within the quark matter. This plasma frequency is generally found to be of the order $\omega_p \sim e\Lambda_{\mathrm{QCD}} \sim 10$ MeV for a wide range of quark matter phases [22]. The muon energy spectrum will therefore be peaked at this energy but may run up to the GeV scale for muons directly produced in annihilations near the surface. Energy loss scales exponentially with the depth at which the muon is produced thus the energy spectrum will be approximated as

$$\frac{dn_\mu}{dk} = \frac{1}{\omega_p} e^{(\omega_p - k)/\omega_p}, \qquad m_p > k > \omega_p, \tag{B1}$$

where k is the muon momentum and m_p is the proton mass. This will be taken as the initial spectrum for muons escaping the nugget.

A muon traveling through the atmosphere will lose energy scattering off the surrounding molecules. As these are neutral on scales larger than a few times the Bohr radius, scattering requires the exchange of photons with an energy above $m_e\alpha$. The cross section for this processes in the limit where $m_\mu \gg m_e\alpha$ is given by

$$\sigma_{\mu,e} \approx \frac{2\pi\alpha}{m_e^2}\frac{1}{v^2} \equiv \sigma_0 v^{-2} \approx 7\times 10^{-23}\,\mathrm{cm}^2\left(\frac{c}{v}\right)^2, \tag{B2}$$

where v is the muon's velocity. This translates to a scattering length of

$$l_s = \frac{1}{\sigma_{\mu,e} n_{\mathrm{at}}(h)}, \tag{B3}$$

where n_{at} is the number density of the atmosphere. Scattering losses are dominated by events involving the lowest possible intermediate energy photon, thus the muon will lose roughly $m_e\alpha$ worth of energy on scattering. A muon with initial kinetic energy $T = E - m_\mu$ will then lose most of its energy after $T/m_e\alpha$ scatterings. Thus the stopping length for a muon of energy E and momentum p will be

$$L_s = \frac{E - m_\mu}{m_e\alpha} l_s = \frac{E - m_\mu}{m_e\alpha}\left(\frac{p}{E}\right)^2 \frac{1}{\sigma_0 n_{at}}. \tag{B4}$$

The other relevant length scale is the typical distance that a muon travels before it decays,

$$L_d = v\gamma\tau_\mu = \frac{p\tau_\mu}{m_\mu}, \tag{B5}$$

where $\tau_\mu = 2.2\times 10^{-6}$ s is the muon lifetime. Once the muon decays to an electron or positron it will rapidly be lost in the electromagnetic component of the shower which this analysis makes no attempt to trace the evolution of. A muon thus travels a distance

$$L(p) = L_d \ \text{ if } L_d < L_s \quad L_s \ \text{ if } L_s < L_d \tag{B6}$$

before its energy is dissipated into the electromagnetic shower. Note that scattering is the dominant stopping process for low momentum particles at large atmospheric densities while decays dominate high in the atmosphere and for higher energy muons. The relevant quantity for what follows is actually the energy averaged length obtained by integrating over the muon spectrum (B1)

$$\bar{L} = \int_{\omega_p}^{m_p} \frac{dp}{\omega_p} L(p) e^{(\omega_p - p)/\omega_p}. \tag{B7}$$

Given the annihilation rate Γ_{an} the total number of particles produced at a given height may be estimated as

$$N(h) = \frac{\Gamma_{\mathrm{an}}}{v_n}\chi_\mu \bar{L}. \tag{B8}$$

This expression will be used in the context of Sec. VI in order to track the evolution of the shower's particle content. Similar considerations can be used to approximate the particle content at the Earth's surface. Under the assumption that particle emission from the nugget is primarily along the nugget's direction of motion the number of muons reaching an area of the surface will be

$$\frac{dN}{dA} = \int_0^\infty \frac{dh}{2\pi(h^2 + b^2)}\frac{\Gamma_{\mathrm{an}}}{v_n}\chi_\mu \mathcal{F}, \tag{B9}$$

where b is the distance from the shower core and $\mathcal{F}$ is the fraction of initial muons which is able to propagate far enough to reach the surface. Both loss mechanisms produce an exponential extinguishing of the initial muon number; the characteristic length scale for this process is given by the energy averaged length in (B7),

$$\mathcal{F} = \exp\left[-\frac{\sqrt{b^2 + h^2}}{\bar{L}}\right]. \tag{B10}$$

The integration of (B9) with this expression for $\mathcal{F}$ is used to approximate the surface flux of the shower.

APPENDIX C: UNDERGROUND DETECTORS

This section briefly discusses the constraints imposed on quark nuggets based on underground detectors. While the muonic shower can be quite extensive in the atmosphere the higher density of rock strongly limits the range over which the muons can travel. This can be seen by replacing the atmospheric density in (B3) with the density of surface rock. In this case the scattering length drops by a factor of at least a thousand and the muons are absorbed quite close to their production site. This is, of course, precisely the reason why such experiments are conducted under a large mass of shielding rock. Thus, the ability to constrain the density of quark nuggets scales almost directly with detector area (or the effective cross section presented by the cavity in which the detector is located). If we apply this to a relatively large detector such as Super-Kamiokande [26] the effective detector size is limited to at most on the order of 100 m^2. In this case, even near the upper limit of the allowed flux ($1/km^2/yr$) one would expect an event rate of only ~ 1/century. As such the detection probability remains small even for experiments with run times of almost a decade.

It should also be noted that most underground experiments work very hard to block the influence of muons produced outside of the fiducial volume of the detector. Given these cuts intended to remove the radioactive decay background only nuggets passing very close to the detector would be capable of generating a sufficiently high muon multiplicity to result in detection.

[1] E. Witten, Phys. Rev. D **30**, 272 (1984).
[2] A. R. Zhitnitsky, J. Cosmol. Astropart. Phys. 10 (2003) 010.
[3] J. Knödlseder *et al.*, Astron. Astrophys. **441**, 513 (2005).
[4] A. Zhitnitsky, Phys. Rev. D **76**, 103518 (2007).
[5] D. H. Oaknin and A. R. Zhitnitsky, Phys. Rev. Lett. **94**, 101301 (2005).
[6] A. W. Strong, I. V. Moskalenko, and O. Reimer, Astrophys. J. **613**, 962 (2004).
[7] K. Lawson and A. R. Zhitnitsky, J. Cosmol. Astropart. Phys. 01 (2008) 022.
[8] M. P. Muno *et al.*, Astrophys. J. **613**, 326 (2004).
[9] M. M. Forbes and A. R. Zhitnitsky, J. Cosmol. Astropart. Phys. 01 (2008) 023.
[10] D. P. Finkbeiner, Astrophys. J. **614**, 186 (2004).
[11] M. M. Forbes and A. R. Zhitnitsky, Phys. Rev. D **78**, 083505 (2008).
[12] J. Abraham *et al.* (Pierre Auger Collaboration) Phys. Lett. B **685**, 239 (2010).
[13] J. Madsen, J. Phys. G **31**, S833 (2005).
[14] V. Springel *et al.*, Nature (London) **435**, 629 (2005).
[15] K. Greisen, Phys. Rev. Lett. **16**, 748 (1966).
[16] G. T. Zatsepin and V. A. Kuzmin, Pis'ma Zh. Eksp. Teor. Fiz. **4**, 114 (1966) [JETP Lett. **4**, 78 (1966)].
[17] B. Fick (Pierre Auger Collaboration), *Proceedings of the 28th International Cosmic Ray Conferences (ICRC 2003), Tsukuba, Japan, 2003* (Universal Academy, Tokyo, 2003).
[18] D. T. Son and M. A. Stephanov, Phys. Rev. D **61**, 074012 (2000); see [27] for this paper's erratum.
[19] M. M. Forbes, K. Lawson, and A. R. Zhitnitsky, Phys. Rev. D **82**, 083510 (2010).
[20] A. Schmidt *et al.*, Nucl. Instrum. Methods Phys. Res., Sect. A **601**, 347 (2009).
[21] P. Belli *et al.*, Phys. Rev. D **61**, 023512 (1999).
[22] C. Alcock, E. Farhi, and A. Olinto, Astrophys. J. **310**, 261 (1986).
[23] J. Madsen, Phys. Rev. Lett. **87**, 172003 (2001).
[24] M. Alford and K. Rajagopal, in *Pairing in Fermionic Systems* (World Scientific, Singapore, 2006).
[25] D. H. Oaknin and A. Zhitnitsky, Phys. Rev. D **71**, 023519 (2005).
[26] Y. Fukuda *et al.*, Nucl. Instrum. Methods Phys. Res., Sect. A **501**, 418 (2003).
[27] D. T. Son and M. A. Stephanov, Phys. Rev. D **62**, 059902 (E) (2000) (erratum to Ref. [18]).